

Comparative molecular dynamics simulations of amphotericin B–cholesterol/ergosterol membrane channels

Maciej Baginski^{a,*}, Haluk Resat^{b,1}, Edward Borowski^a

^aDepartment of Pharmaceutical Technology and Biochemistry, Chemical Faculty, Technical University of Gdansk, Narutowicza St. 11, 80-952 Gdansk, Poland

^bDepartment of Physics, Koç University, Rumelifeneri Yolu, Sariyer Istanbul, Turkey

Received 27 March 2002; received in revised form 22 July 2002; accepted 3 September 2002

Abstract

Amphotericin B (AmB) is a very effective anti-fungal polyene macrolide antibiotic whose usage is limited by its toxicity. Lack of a complete understanding of AmB's molecular mechanism has impeded attempts to design less toxic AmB derivatives. The antibiotic is known to interact with sterols present in the cell membrane to form ion channels that disrupt membrane function. The slightly higher affinity of AmB toward ergosterol (dominant sterol in fungal cells) than cholesterol (mammalian sterol) is regarded as the most essential factor on which antifungal chemotherapy is based. To study these differences at the molecular level, two realistic model membrane channels containing molecules of AmB, sterol (cholesterol or ergosterol), phospholipid, and water were studied by molecular dynamics (MD) simulations. Comparative analysis of the simulation data revealed that the sterol type has noticeable effect on the properties of AmB membrane channels. In addition to having a larger size, the AmB channel in the ergosterol-containing membrane has a more pronounced pattern of intermolecular hydrogen bonds. The interaction between the antibiotic and ergosterol is more specific than between the antibiotic and cholesterol. These observed differences suggest that the channel in the ergosterol-containing membrane is more stable and, due to its larger size, would have a higher ion conductance. These observations are in agreement with experiments.

© 2002 Elsevier Science B.V. All rights reserved.

Keywords: Amphotericin B; Cholesterol; Ergosterol; Phospholipid; Molecular modeling; Ion channel

1. Introduction

Amphotericin B (AmB) is a polyene macrolide antibiotic (Fig. 1a) that has been used as a “golden” standard drug to treat systemic fungal infections for more than 40 years. Despite its severe side effects, and particularly its nephrotoxicity, it is still the drug of choice used to treat advanced infections due to the lack of better alternatives [1–4]. Systemic fungal infections are often observed as side effects in chemotherapy treatments which impair the immune system, and therefore, finding new anti-fungal drugs or improving old standards is an important emerging problem [4–6]. Unlike other anti-fungal drugs, AmB does not generate opportunistic resistance in fungal strains [3]. This desirable property further enhances AmB's medical importance. Due to these reasons,

the design of less toxic derivatives or formulations has important medical implications. Some successful results concerning lipid or liposome AmB formulations have been introduced recently (see, e.g., the review in Ref. [7]). However, such approaches are too expensive for a typical medical treatment, therefore limiting their usage.

AmB's molecular mechanism of action is still not understood well enough to make rational design of new derivatives possible. It is known that AmB interacts with the components of cell membrane and forms ion channels [8–11]. These ion channels disrupt membrane functions and cause uncontrolled cation transport through the membrane that eventually leads to cell death. According to the widely accepted sterol hypothesis [12,13], presence of sterol molecules in the membrane is necessary for AmB to be able to form conducting ion channels in cell membranes. It has been observed that AmB can also form conducting channels when there are no sterols in the membrane [14]. However, the level of the antibiotic concentration needed to observe conductance in these latter channels is much higher than

* Corresponding author. Tel.: +48-58-3471596; fax: +48-58-3471144.

E-mail address: maciekb@hypnos.chem.pg.gda.pl (M. Baginski).

¹ Current address: Pacific Northwest National Laboratory, P.O. Box 999, MS: K1-83, Richland, WA 99352, USA.

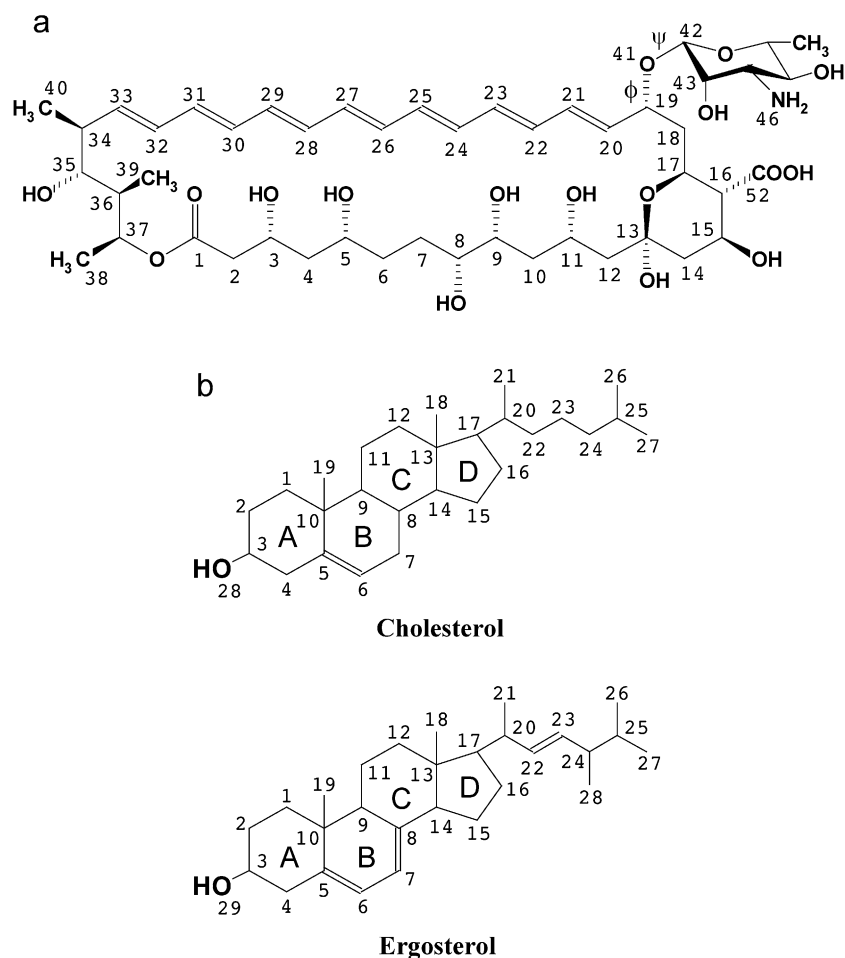


Fig. 1. (a) Structure of the antibiotic AmB with partial atom numbering. (b) Structure of cholesterol and ergosterol with atom numbering.

required under physiological conditions. Therefore, it is very unlikely that such channels would be formed under the physiological *in vivo* conditions.

Chemotherapeutic application of AmB is based on the slightly higher (or different) affinity of the antibiotic towards ergosterol-containing membranes (fungal cells) than cholesterol-containing membranes (animal cells) [13,15,16]. Unfortunately, the affinity of AmB toward cholesterol molecules is not negligible and this interaction is responsible for the severe toxicity of the antibiotic. There are only minor structural differences between cholesterol and ergosterol (Fig. 1b). Why and how these differences may lead to higher AmB–ergosterol (AmBER) than AmB–cholesterol (AmBCh) affinity were only hypothesized [17,18]. It was postulated that the molecular structure of ergosterol better complements that of AmB [19] and that the presence of additional carbon–carbon double bonds strengthens the electrostatic interaction between ergosterol and AmB molecules [20,21]. One may also postulate that small structural differences lead to small differences of interactions between AmB and sterol molecules. However, since many AmB molecules are involved in the formation of a single membrane channel, cumulative effect of such small differences

can have a significant influence on the stability of the channel. The importance of structural features of sterols for AmB activity is further supported by experiments showing that AmB-resistant fungal strains contain modified sterols, which have structures very similar to that of ergosterol, in their plasma membrane [3].

It is known that AmB can form two types of channels: single-length channel (SLC) and double-length channel (DLC) [22,23]. DLC is simply a channel where two SLC are arranged in a tail-to-tail configuration. Formation of DLC channels was observed when the antibiotic is added from both sides of the membrane. Administering AmB only from one side of the membrane results in the SLC formation. In clinical usage AmB is added to the medium in which the cells are present (i.e., they have access to the cell membrane only from one side). Therefore, it is reasonable to assume that SLC-type membrane ion channels are formed during the regular medical usage. Since it is more relevant, single-length AmB membrane channel was chosen as the subject matter of our study.

AmB's mechanism of action has been studied experimentally for several decades (e.g., Refs. [8–11,15]). Theoretical studies using various computational chemistry methods were

also pursued [19–21,24–34]. Progress in molecular modeling methods as well as the developments in computer technology made it possible to study lipid bilayer and membrane channel systems at the atomic level (see, e.g., recent reviews in Refs. [35–37]). This progress allows for the use of theoretical studies at the molecular level to supplement experiments.

The present work is a continuation of our earlier molecular modeling study of the SLC type AmB-channel in a cholesterol-containing membrane [32]. In this work we test the sterol hypothesis that the affinity difference of AmB towards fungal and animal cells (whose sterol contents are different) is due to the differences in the interactions between AmB and the sterols at the molecular level. SLC-type model AmB membrane channels formed in cholesterol- and ergosterol-containing phospholipid bilayers are studied using molecular dynamics (MD) simulations. Since there is no experimental evidence that the stoichiometry of the channels would be different, it is assumed that both channels have the same AmB–sterol stoichiometry and topology. Because of these assumptions, it can be expected that the differences between the properties of the two channels would largely be due to the differences between AmB's pattern of interaction with the sterols cholesterol and ergosterol. As discussed below, we have observed several noticeable differences between the channel structures in our modeling study. The most significant difference is that the diameter of the AmBER channel is larger than the AmBCh channel. It was also found that the AmB channel in the ergosterol-containing membrane has a more pronounced pattern of intermolecular hydrogen bonds and that the interaction between AmB and ergosterol is more specific than the antibiotic's interaction with cholesterol. How and why the observed differences can be helpful in explaining the affinity difference are also discussed.

It is also worth mentioning that our comparative studies of AmB channels in membranes containing cholesterol or ergosterol can be regarded as a pilot one for future studies of channels built from other AmB derivatives. According to biophysical and biological studies of less toxic AmB derivatives, formation of the membrane channels and their stability are hypothesized as essential factors responsible for better chemotherapeutic properties of these new AmB derivatives [38–40].

2. Methods

2.1. Molecular models of studied channels

Even though the molecular structures of AmB and of cholesterol and ergosterol were determined long time ago [41–43], the macromolecular structure of the AmB channel has not yet been obtained experimentally. Nevertheless, several realistic models of the AmB membrane channel have been proposed and the predicted properties of these channels are highly supported by experimental evidences

[8,23,25,27,32,33,44–49]. In these proposed and/or studied models, which are highly similar, the chain of hydroxyl groups of AmB (Fig. 1a) faces towards the channel pore, and the conjugated double bond chains are positioned next to the membrane sterols and lipids. Such an orientation of the antibiotic molecules is also supported by recent studies of the amphipathic/amphiphilic pattern of AmB molecule [20] and AmB-like isosterical molecules [50].

Our AmB–sterol channel closely resembles the models suggested earlier by various groups [32]. Each AmB–sterol channel consists of eight AmB molecules and eight sterol molecules which are noncovalently associated. The channels are surrounded by 34 dimyristoylglycerophosphatidylcholine (DMPC) (17 in each monolayer) molecules which represents the model bilayer membrane. This channel/lipid complex has a cylindrical shape and its both sides, as well as the interior of the channel pore, are solvated using a total of 1666 water molecules at the bulk water density. We have studied the same model of AmBCh channel previously [32,51]. To make the two simulations compatible, the starting structure of the studied AmBER channel was constructed by replacing the cholesterol with ergosterol molecules in the starting structure of AmBCh channel.

2.1.1. AmBCh channel

Being an amphoteric and amphipathic molecule (Fig. 1a), AmB forms channels in which its hydrophilic hydroxyl groups point toward the channel's pore. Its hydrophobic part, the chain of conjugated carbon–carbon double bonds, interacts with surrounding lipids and is buried within the lipid bilayer. The diameter of the channel is estimated to be in the 7–10 Å range [52]. In the model used in this study, there are eight molecules each of AmB and the sterols. These molecules are symmetrically placed around a cylindrical pore where neighboring AmB molecules form V-shaped wedges. Sterol molecules occupy these wedges. The phospholipid molecules surround the AmB–sterol complex forming the membrane bilayer. Details of how the AmBCh channel was constructed and placed in a pre-equilibrated box of DMPC phospholipids [53] may be found in Ref. [32]. We have repeated and extended the MD simulations that were communicated earlier [32]. In this report we convey the results of these new simulations. We have started with a configuration of DMPC molecules which was already equilibrated [32]. To relieve the stress due to the possible misplacements in the starting symmetric structure of AmBCh, the positions of the DMPC and water molecules were optimized first using 500 steps of steepest descent followed by 1000 steps of conjugated gradient methods. AmB and cholesterol molecules were fixed during this initial optimization. This AmBCh system was further equilibrated (detailed in Section 2.2) before collecting the simulation data.

2.1.2. AmBER channel

To form the AmBER channel, eight cholesterol molecules in the starting structure of the AmBCh channel were

replaced with eight ergosterol molecules. This approach preserved the similarity between the starting structures of AmBCh and AmBER channels and allowed for better comparison of the simulation results. To obtain a physically relevant initial structure, unphysical structural strains in the starting configuration of the AmBER channel was relieved by geometry optimization using 1000 steps of steepest descent followed by the 6000 steps of conjugated gradient methods. During this initial optimization, AmB and ergosterol molecules were fixed and only DMPC and water molecules were allowed to relax. The channel structure was later further equilibrated using short MD runs.

2.2. MD simulations

AmBCh and AmBER simulations were performed in a very similar manner. All geometry minimization and MD simulations were performed using the CHARMM molecular simulation program [54]. The bond, angle, dihedral, van der Waals, and electrostatic terms were included in defining the interaction potentials. With the exception of the AmB and sterols (CHARMM ver. 22), interaction force field parameters were taken from the CHARMM potential library version 25 β 1 that also contains parameters for lipids [55]. The AmB and sterol site charges were taken from our earlier study [20] where partial charges were derived using molecular electrostatic potential fits. The TIP3P model [55,56] was chosen to represent the water molecules, and its parameters were taken from CHARMM force field version 25 β 1.

A group-based cutoff was used to truncate the non-bonded van der Waals and electrostatic interactions. Each AmB and sterol was treated as a separate fragment. DMPC molecules were partitioned into 28 fragments using the CHARMM program topology-grouping scheme [55]. In the CHARMM program, group-based truncations are determined using the distance between the molecular centers of the group. As in our earlier study [32], a large cutoff distance of 25 Å was used. This large value of cutoff was tested before [32] and was chosen as necessary to include the interactions between any two AmB and sterol molecules in the channel. The truncation was implemented using a smoothing switch function starting from the distance of 22 Å. The non-bonding interaction pair list was updated every 50 steps. The time step was 2 fs. Hydrogen atom covalent bond lengths were restrained using the SHAKE algorithm with a tolerance of 10^{-6} Å. Constant volume and temperature conditions were used.

To maintain an adequate solvation pattern and to keep the phospholipid bilayer intact, cylindrical and planar restraints were imposed on the water molecules and lipids in both systems. Harmonic mean field restraint potentials as implemented in the CHARMM program were used for this purpose [57]. An imposed mean field potential with a force constant of 30 kcal/mol/Å² restrained the water molecules (i.e. water oxygen atoms) to stay inside a symmetrically placed cylinder with diameter and height of 27 and 54 Å, respectively. Similarly, DMPC molecules were restrained

with a force constant of 30 kcal/mol/Å² to stay within a 30-Å diameter cylinder. No height restraints were necessary for the lipid molecules.

After the initial energy minimization of the lipid and water molecule positions, both simulation systems were further equilibrated in several steps before data collection. The AmBCh and AmBER channel systems were first heated to 300° K in 2 ps. Then system in AmBCh was equilibrated for 102 ps. During the first 32 ps of this equilibration, AmB and cholesterol molecules were constrained to allow for better equilibration of the somewhat arbitrarily placed water and DMPC molecules. The equilibration run was continued for 120 ps in the AmBER simulation. AmB and ergosterol molecules were constrained during the first 60 ps of this equilibration. The equilibration stage for AmBER took longer because, since its tail chain has one more methyl group, ergosterol molecules needed more time to relax. The data collection MD simulations were run for 250 ps for both cases. MD trajectory was saved at 0.4-ps intervals for later use; overall 625 snapshots were recorded for analysis of the results in each case. Both AmBCh and AmBER simulations were performed on a parallel Cray T3E computer. Using 16 nodes, each 250-ps MD simulation took approximately 64 CPU hr.

The time scale of our simulation, 250 ps, is too short to allow for the observation of major changes, such as the formation or destruction of the channels or any large conformational changes such as conversion between the open and closed channel forms. To observe such changes, duration of the simulations should be micro- or even milliseconds. Unfortunately, the associated costs prohibit such simulations. However, the time scale of our simulations is reasonably long enough to investigate the structural properties of the AmB channels at the microscopic level, and performed simulations allowed us to find if there are structural differences that could be responsible for the presumably higher stability of AmBER channel than the AmBCh channel. We would like to note that, to the best of our knowledge, there is only one published report concerning MD simulation of the phospholipid membrane with ergosterol [58], and there are no MD studies of AmB membrane channels where different sterols were used. Therefore, although it employs somewhat short 250-ps simulations, this study attempts such comparative investigation for the first time. The experience gained in this study will be very useful in improving the design of future simulations with promising AmB derivatives.

3. Results and discussion

The MD simulation trajectories were analyzed to emphasize the differences in structural and dynamical properties of AmBCh and AmBER channels. The analysis focused on investigating which intermolecular and intramolecular factors are important for channel's stability and its functional

behavior. To have a better understanding of the range of dynamical motions or structural properties, in addition to calculating the averages, investigated properties were also computed for each molecule or pair of molecules individually. It should be noted that figures which report single molecule properties, (Figs. 3, 7, 9 and 10a,b), contain eight plots, one for each of the eight AmB or sterol molecules in the system.

3.1. Intramolecular properties

3.1.1. Conformation of AmB molecules

The lactone ring of the AmB molecules forming the channel is quite rigid due to the presence of seven conjugated carbon–carbon double bonds. As in our previous simulation

[32], only a limited conformational freedom can be observed for the C6–C7 carbon bond (data not shown). Of the carbon atoms in this part of the lactone ring, only C6 and C7 do not have hydroxyl substituents (Fig. 1a); this lack of hydroxyl substituents allows for the *trans*–*gauche* transformation around the C6–C7 carbon bond. Orientation of the hydroxyl substituent at C8 is opposite to the orientations of the substituents at the neighboring carbon atoms. This difference, and the possibility of having a *trans* C6–C7 bond, makes it possible for the hydroxyl at the C8 position to form intermolecular hydrogen bonds with the hydroxyl groups at the C5 or the C9 positions of the adjacent AmB molecules. On the other hand, a *gauche* C5–C6–C7–C8 conformation allows for the formation of an: (i) intramolecular hydrogen

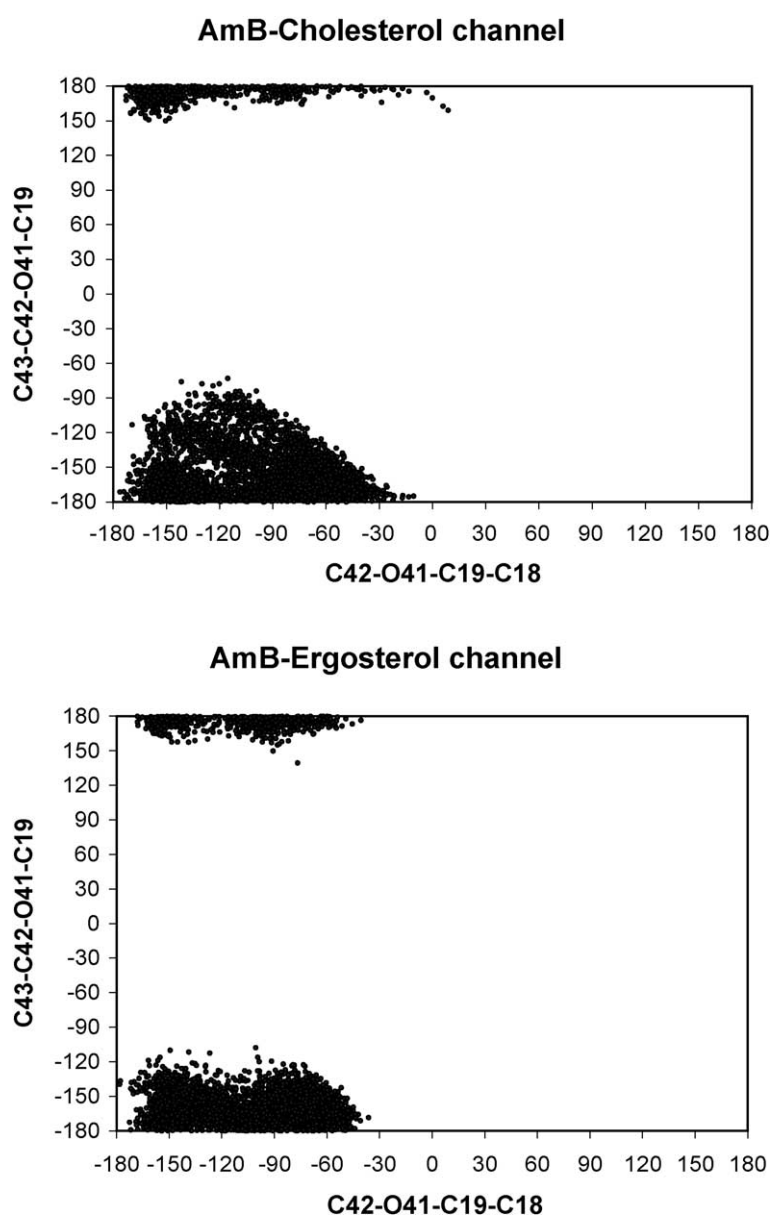


Fig. 2. Distribution of $\phi = \text{C42-O41-C19-C18}$, $\psi = \text{C43-C42-O41-C19}$ dihedral angles of AmB. Each point corresponds to one snapshot from the MD trajectory and to one AmB molecule (8 molecules \times 625 frames = 5000 total data points). Top: AmBCh channel; bottom: AmBEr channel.

bond between hydroxyl groups at the C5 and C8 atoms, and/or (ii) intermolecular hydrogen bond between hydroxyl group at the C5 and C9 atoms of two neighbor AmB molecules. Based on the observation that the *trans*–*gauche* transformations around the C6–C7 bond are less frequent, it can be deduced that AmB's lactone ring is slightly more rigid

in the AmB_{Er} channel. However, in the case of AmB_{Ch} channel, more AmB molecules have the *gauche* conformation for C6–C7 bond than in AmB_{Er} channel. It was also observed that even though the lactone ring is quite restricted, this ring has some flexibility along the conjugated carbon–carbon double bonds. Although this heptaenic system is quite

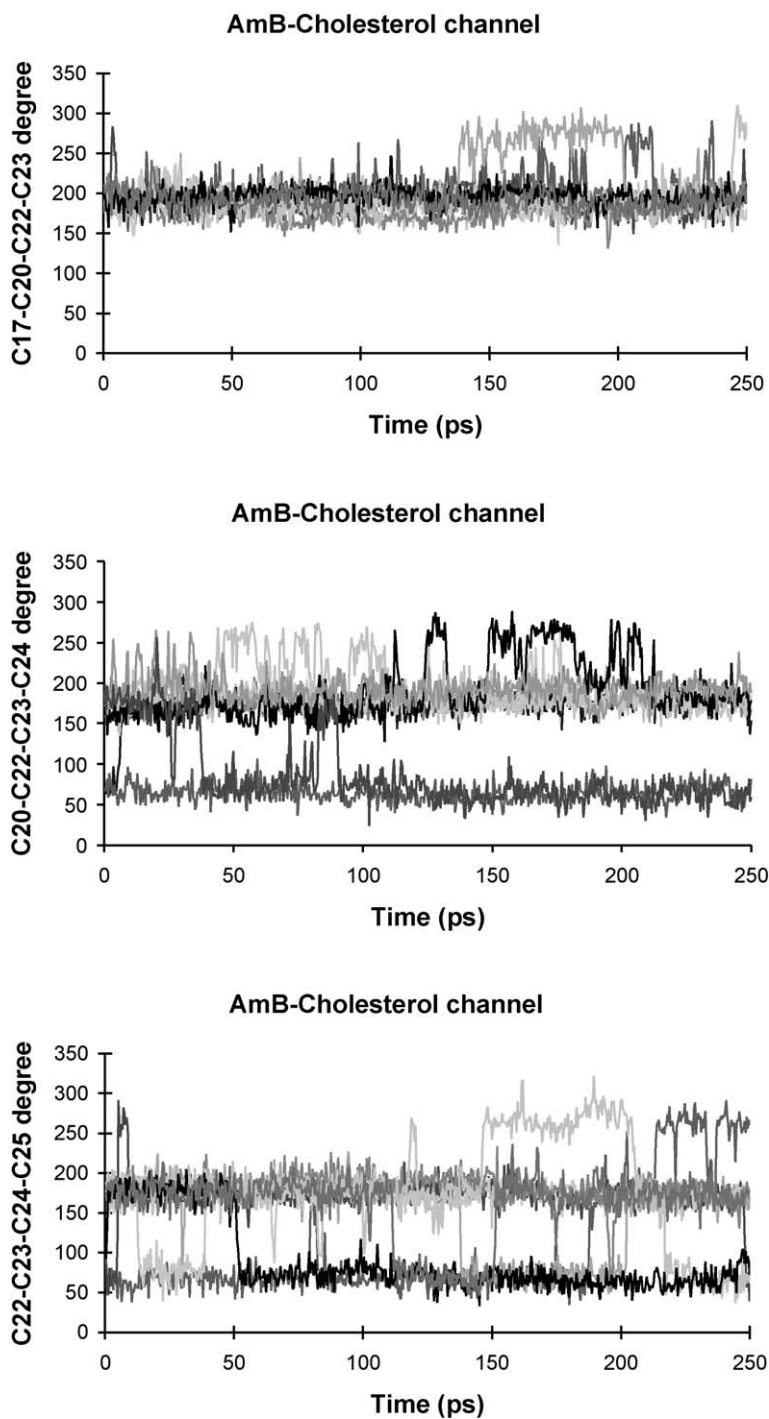


Fig. 3. Change in the cholesterol dihedral angle C17–C20–C22–C23, C20–C22–C23–C24, and C22–C23–C24–C25 as a function of time in the AmB_{Ch} channel. For comparison, bonds C20–C22 and C23–C24 that are adjacent to the carbon–carbon double bond C22–C23 have the *trans* conformation in the ergosterol tail chain (data not shown). Each one of the eight lines corresponds to an individual sterol molecule.

rigid, due to its long length, there is a slight uniform twisting. This twisting of the double bond chain was observed in both of the AmB–sterol simulations (data not shown).

The main difference between two channels concerning the conformational properties of the AmB molecules is in the fluctuation of φ , ψ dihedral angles, where $\varphi \equiv \text{C42–O41–C19–C18}$ and $\psi \equiv \text{C43–C42–O41–C19}$ (Fig. 1a). These angles determine how the amino-sugar moiety is positioned with respect to the macrolide's lactone ring. As was shown before [32,34], the configurations are largely dominated by two conformers (Fig. 2): (i) “open” ($\varphi \approx -150^\circ$, $\psi \approx -180^\circ$), and (ii) “closed” ($\varphi \approx -60^\circ$, $\psi \approx -180^\circ$) forms. In the “open” conformer, the sugar moiety's amino and carboxyl groups are positioned such that they have the ability to form intermolecular hydrogen bonds with the complementary carboxyl and amino groups of the neighboring AmB molecules. Such interactions allow for the formation of a hydrogen bond chain at the entrance of the pore and stabilize the channel [32]. On the other hand, the “closed” conformation is responsible for the formation of intramolecular hydrogen bonds between the carboxyl and the amino groups. Since the AmB molecules are not covalently associated, the “closed” conformer does not contribute to channel's stability. A strong correlation between the (φ , ψ) distribution and the biological activity was observed in our recent molecular modeling studies of AmB amide derivatives [34]. Distribution of the (φ , ψ) angles derived from MD trajectories of both channels (Fig. 2) clearly show that the amino-sugar moiety has more freedom of movement in the AmBCh channel. As a consequence, intermolecular hydrogen bonds between the amino and carboxyl groups may form less efficiently (with a shorter lifetime) in the case of the AmBCh channel. In the case of AmBER channel only two clearly defined conformers are observed (Fig. 2).

3.1.2. Conformation of sterol molecules

The main structural difference between cholesterol and ergosterol appears in the hydrophobic tail (Fig. 1b). Therefore, selected dihedral angles in the tail were monitored.

This analysis confirmed that the rotation around the bonds adjacent to the C22=C23 double bond in ergosterol is hindered. The values of the C17–C20–C22–C23 and C22–C23–C24–C25 angles are 240° and 120° , respectively. Thus, the bonds C20–C22, C22=C23, and C23–C24 in the tail of ergosterol have *trans* conformations throughout the simulation (data not shown). In contrast, the same tail bonds of cholesterol are not always in *trans* conformation (Fig. 3). Therefore, compared to cholesterol's tail, ergosterol's tail chain is stiffer and more elongated. This difference is particularly obvious when the temporal behavior of the C22–C23 and C23–C24 bonds are analysed. Fig. 3 shows that during simulation, conformations of the studied bonds of the cholesterol change often in between *trans* and *gauche* angles. These results are in agreement with our previous conformational studies of isolated cholesterol and ergosterol molecules [19]. The rigidity of the ergosterol tail chain increases its short range van der Waals contact with the AmB and can contribute to the stability of the whole channel. These MD results support the hypothesis that small structural differences between cholesterol and ergosterol could lead to important differences in AmB–sterol interactions.

3.1.3. Intramolecular hydrogen bonds

In order to find if there are qualitative differences between AmBCh and AmBER channels in their ability to form intramolecular hydrogen bonds, the behavior of all eight AmB molecules was individually tracked. Bonds having all of the following three features were included in the statistics: (i) the distance not longer than 3.3 Å between donor and acceptor polar atoms (oxygen or nitrogen), (ii) the distance not longer than 2.1 Å between acceptor polar atom and hydrogen atom, and (iii) the planar acceptor–hydrogen–donor angle between 90° and 180° . The statistical distribution of intramolecular hydrogen bonds is presented in Fig. 4. Although there are small differences, the overall shape of intramolecular hydrogen bond distribution is very similar for both channels. AmBCh channel exhibits only a slightly higher

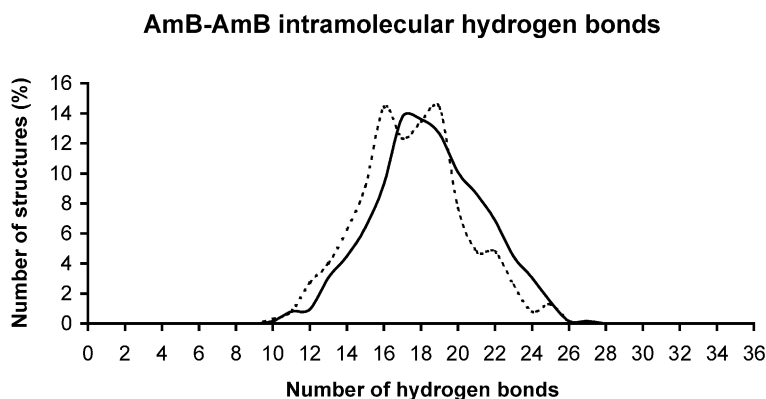


Fig. 4. Distribution of the total number of AmB intramolecular hydrogen bonds. Each line indicates the percentage of structures (frames) from MD simulation trajectory having a particular number of hydrogen bonds (indicated on axis X). AmBCh channel (solid line); AmBER channel (dashed line).

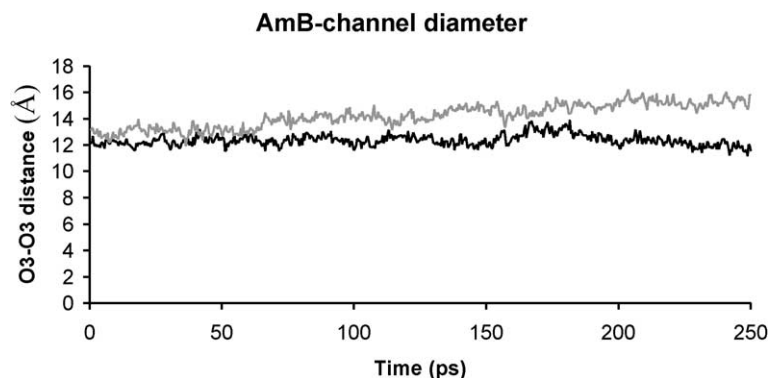


Fig. 5. The distance between O3 oxygen atoms of two AmB molecules placed across from each other in the pore. This distance is a reasonable measure of the pore diameter in the narrowest part of the channel. AmBCh channel (lower dark line); AmBER channel (upper light line).

number of hydrogen bonds compared to AmB–ergosterol channel.

3.2. Intermolecular properties

3.2.1. Overall properties of the channel

The most important biophysical feature of the channel is possibly its pore size. Knowing the pore diameter can be helpful in deducing if the channel is in its open or closed state and if it can limit ion passage. The interplay between AmB diameter and ion passage was analyzed in a previous

study [51]. Since AmB hydroxyl groups point towards the channel pore and may interact with the passing ions, the distance between the hydroxyl groups of the AmB molecules oppositely placed across the pore in the narrowest part of the channel is a good measure of the pore diameter of the channel. Four such distances were defined by pairing the eight AmB molecules. The average value of these distances as a function of time is presented in Fig. 5. The reported distances are between the hydroxyl groups at AmB's C3 positions. This level corresponds to the narrowest part of the channel [29,32]. Comparison of the results indicates that the

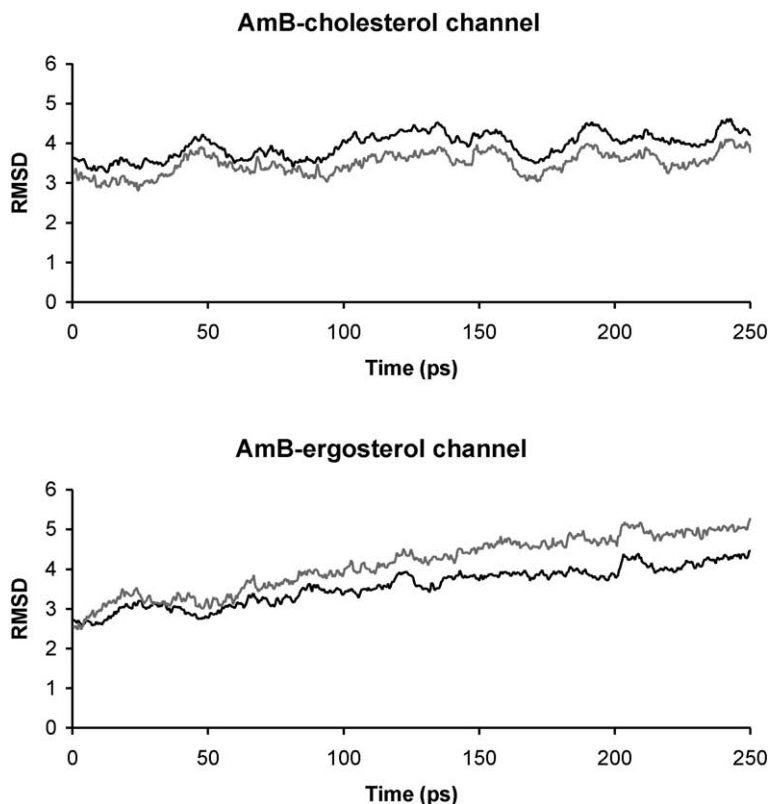


Fig. 6. Upper panel: Change of RMSD for AmB (dark line) and cholesterol (light line) molecules as a function of time in the AmBCh channel. Lower panel: Change of RMSD for AmB (dark line) and ergosterol (light line) molecules as a function of time in the case of AmBER channel.

AmBER channel is slightly wider than the AmBCh channel (Fig. 5). Since the conductance of the channel is roughly proportional to the square of the diameter, because of its larger size, it can be estimated that the ionic conductance would be higher in the AmBER channel. The narrower AmBCh channel may have increased interaction strength between the AmB molecules, and the hydroxyl groups in the narrowest part may cause stronger friction effects on the movement of the ions. It was also found that AmBCh has a more symmetrical shape. We hypothesize that this difference is due to different interaction of the channel with surrounding sterols—cholesterol or ergosterol (see the detailed discussion of these interactions below).

Another property describing the overall behavior of the channel is the root mean square deviation (RMSD) of the molecules. The RMSDs as a function of time were calculated for each AmB and sterol molecule separately and then averaged for each type of molecules (Fig. 6). The RMSD values were computed by superimposing the MD snapshot configurations to the initial symmetric structures of the AmBCh and AmBER channels. In the case of the AmBCh channel, there were some periodic fluctuations, but all AmB molecules had comparable RMSDs. The RMSD values of

the cholesterol molecules in AmBCh channel were comparable to the RMSD of the AmB molecules. Periodic fluctuations (with cycle times of 25–50 ps) are indicators of AmBCh channel's "breathing" motion. These fluctuations reduce the "effective diameter" of the pore.

On the other hand, the RMSD of the molecules has a larger variation in the AmBER channel (data not shown). Unlike the AmBCh case, there is no observed periodicity in the RMSD distribution of the AmBER channel (Fig. 6). However, close inspection of Fig. 6 shows that the motion of an AmB molecule and the ergosterol molecules that are in paired contact with it are correlated. This may indicate that the ergosterol and AmB molecules pair up better and move more in concert with each other.

3.2.2. Intermolecular hydrogen bonds between AmB molecules

Having many polar groups, AmB is prone to form intermolecular hydrogen bonds. A chain of intermolecular hydrogen bonds between AmBs in a channel-forming configuration was observed in our previous study using a 60-ps MD simulation [59]. The results of the 250-ps MD simulation communicated in this report and the results of our

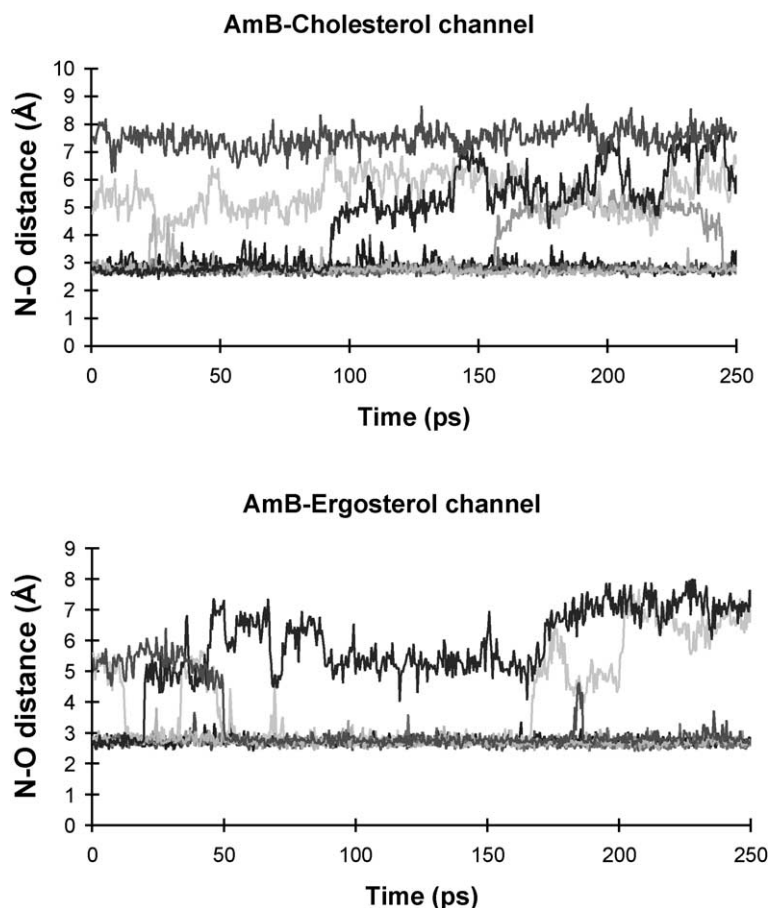


Fig. 7. Number of intermolecular hydrogen bonds formed between amino and carboxyl groups of two neighboring AmB molecules. Each of the eight lines corresponds to one pair of AmB molecules. AmBCh channel (upper panel); AmBER channel (lower panel).

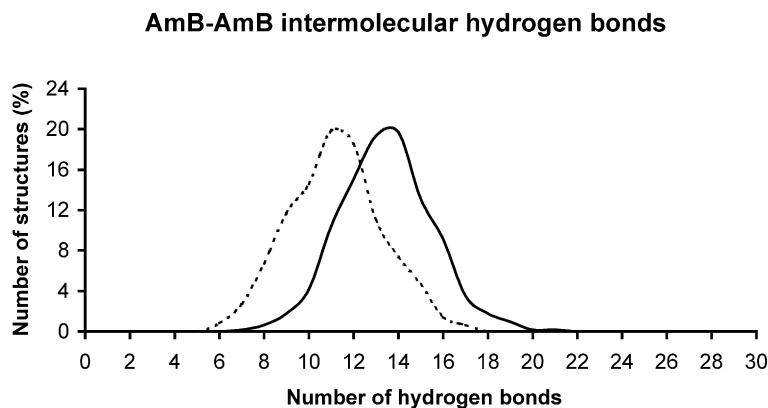


Fig. 8. Distribution of the total number of intermolecular AmB–AmB hydrogen bonds. Each line indicates percentages of structures (frames) from the MD simulation trajectory having a particular number of hydrogen bonds (x-axis). AmBCh channel (solid line); AmBER channel (dashed line).

earlier much shorter simulation of the AmBCh channel are mostly in agreement. The most notable difference is that in the earlier simulation a chain of intermolecular hydrogen bonds was observed in the central part of the channel between the hydroxyl groups of the C8 and C9 sites of the neighboring AmB molecules [59]. The longer MD simulation results do not entirely confirm this observation: The chain of intermolecular hydrogen bonds was observed only at the beginning of the simulation (data not shown),

and the hydrogen bond chain broke after about 50 ps. In the AmBER channel, the chain of intermolecular hydrogen bonds between the hydroxyl groups of the C8 and C9 sites did not form at all. The analysis of the MD data also did not indicate formation of any other stable intermolecular hydrogen bond chain in the central part of the channel. However, it was observed that the C8 and C5 hydroxyl groups form stable intramolecular hydrogen bonds in both AmBCh and AmBER channels (data not shown).

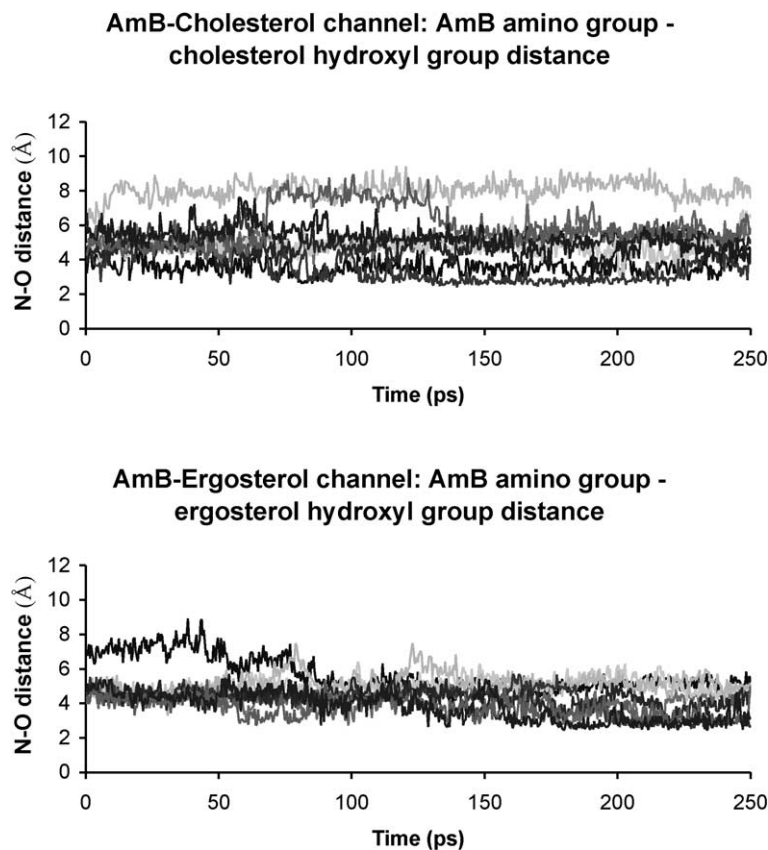


Fig. 9. Number of AmB–sterol hydrogen bonds between the AmB amino group and the closest sterol hydroxyl group as a function of time. Each one of the eight lines corresponds to a pair of AmB–sterol molecules. AmBCh channel (upper panel); AmBER channel (lower panel).

As observed in our previous study [59], a proper conformation of the amino-sugar ring allows for the formation of intermolecular hydrogen bonds between carboxyl and amino groups of the amino-sugar moieties of neighboring AmB molecules. Although both AmBCh and AmBER channels have this chain of intermolecular hydrogen bonds, their tendency for forming the bond chain is not the same. In the AmBER channel, the intermolecular hydrogen bonds between amino and carboxyl groups are present on average for seven out of eight pairs of AmB molecules (Fig. 7). In comparison, this hydrogen bond chain is much weaker in the AmBCh channel; at most, four out of eight such bonds are present at the same time (Fig. 7). This is an important finding because, since it has a larger pore size, one would expect AmBER channel to have less stable intermolecular hydrogen bonds between the AmB molecules. Apparently, a slightly larger pore size (as in the AmBER channel) makes it possible for the amino and carboxyl groups of the neighboring AmB mole-

cules to couple better and form more steady intermolecular hydrogen bonds. Since intermolecular hydrogen bonds between adjacent AmB molecules are essential for channel stability, one may conclude that AmBER is more stable. It should be noted that the amino and carboxyl groups of the amino-sugar moiety are the usual targets for chemical modifications of AmB, and the derivatives with bulky substituents at these positions exhibit very different chemotherapeutic properties concerning toxicity [34,38,60]. The difference in the ability to form intermolecular hydrogen bonds that can stabilize the channel may be responsible for the differences in the biological properties of the two studied channel types.

The distribution of the total number of intermolecular hydrogen bonds is presented in Fig. 8. The criteria used above to define intramolecular hydrogen bonds were also used in computing the reported intermolecular hydrogen bond distribution. The distributions for the AmBCh and AmBER channels are very similar except that there is a small

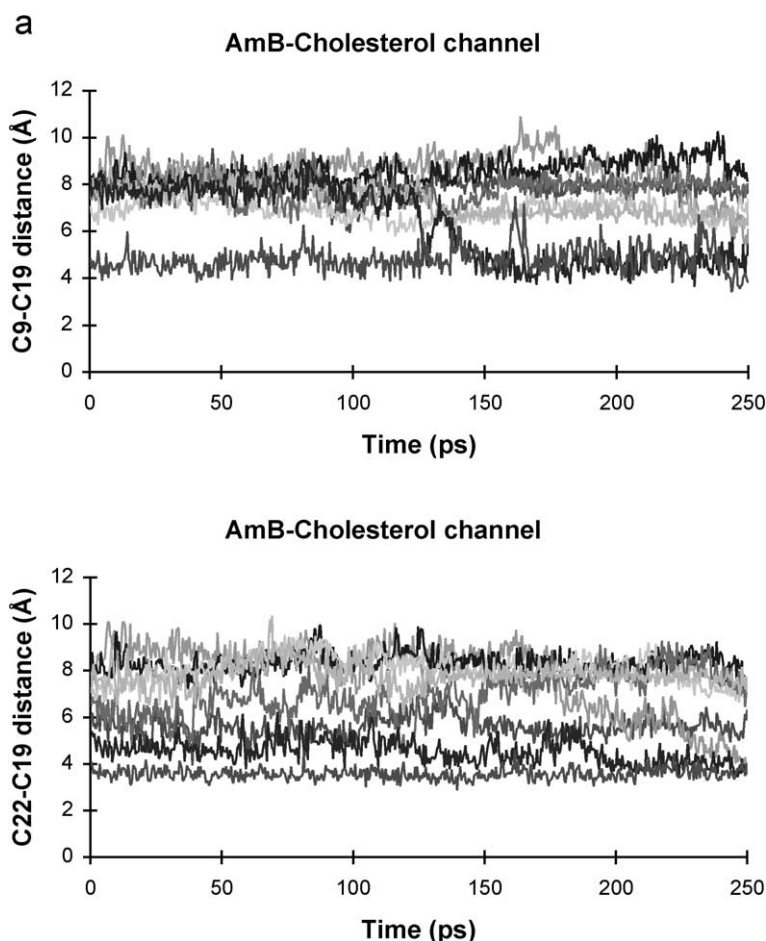


Fig. 10. (a) Relative position of cholesterol and AmB molecules in the AmBCh channel as a function of time. Upper panel: Distance between AmB's C9 carbon atom and sterol's C19 carbon atom. Lower panel: Distance between AmB's C22 carbon atom and sterol C19 carbon. (b) Relative position of ergosterol and AmB molecules in the AmBER channel as a function of time. Upper panel: Distance between AmB's C9 carbon atom and sterol's C19 carbon atom. Lower panel: Distance between AmB's C22 carbon atom and sterol C19 carbon. (c) Distribution of channel structures in the simulation with asymmetric position of sterol molecule relative to AmB. Number of asymmetric AmB–sterol pairs (out of possible 8) in each MD frame is presented on axis *X*. Number of snapshots with a defined asymmetric number of AmB–sterol pairs is presented on axis *Y*. The AmB–sterol pair was regarded as asymmetric when the distance C9–C19 and C22–C19 differed by more than 2 Å. AmBCh channel (solid line); AmBER channel (dashed line).

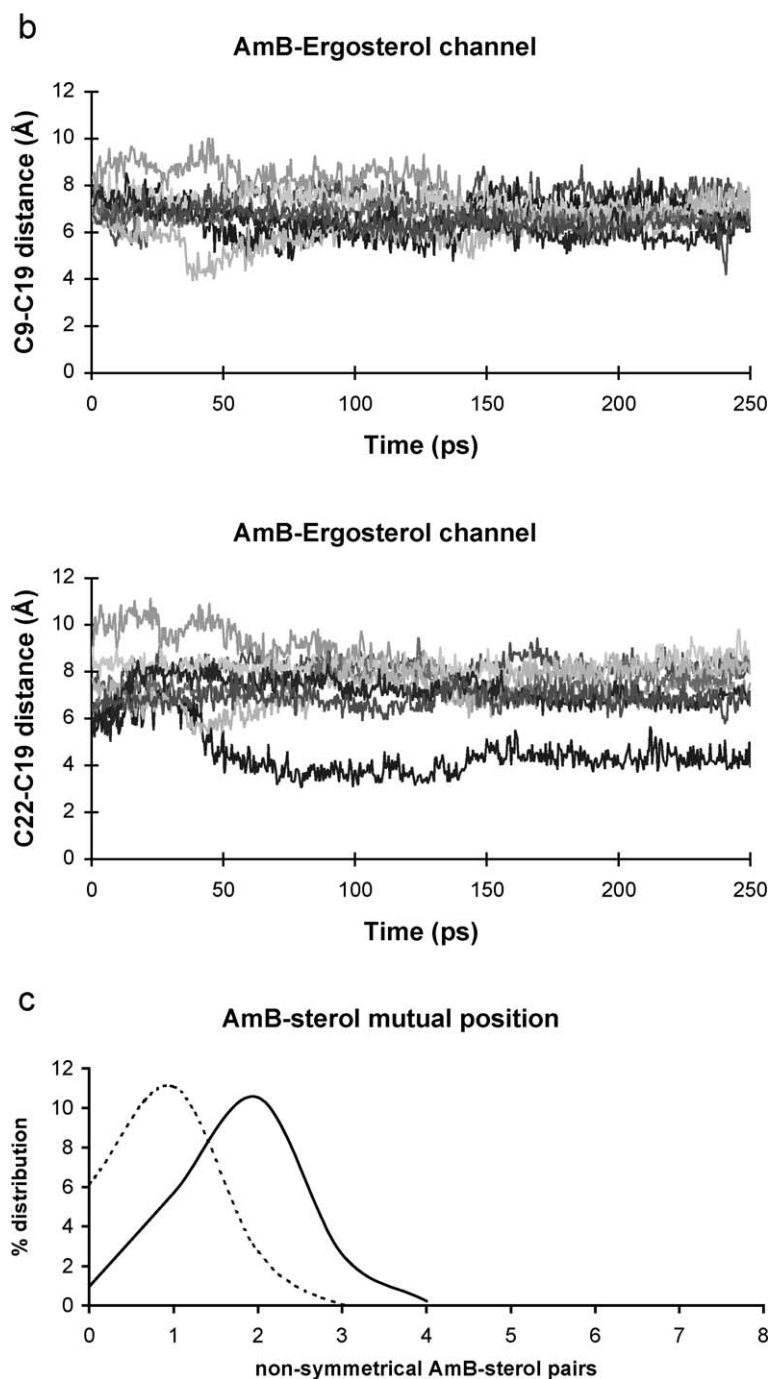


Fig. 10 (continued).

shift in the peak position. On average, the AmBER channel has a slightly lower number of hydrogen bonds between AmB molecules. This difference is most likely due to the difference between the pore size of both channels. Being slightly smaller, the distance between the AmB molecules would be shorter in the AmBCh channel. This may help in the formation of more hydrogen bonds between adjacent AmB molecules. It has to be kept in mind that the contribution of hydrogen bonds to the stability of the channel

would be proportional to the total number of hydrogen bonds. Although the AmBCh channel has a larger number of intermolecular AmB–AmB hydrogen bonds, because of the slight size difference, it also has less number of other types of hydrogen bonds than the AmBER channel. As reported below, the latter types of hydrogen bonds are more abundant and dominate the total tally, and therefore, overall hydrogen bonding contribution to the structural stability is larger in the AmBER channel.

3.2.3. Intermolecular hydrogen bonds between AmB and sterol molecules

Two types of hydrogen bonds were postulated to play a key role in the AmB–sterol interaction [17]: hydrogen bonds (i) between sterol hydroxyl group and amino group of AmB molecule, and (ii) between sterol hydroxyl group and carboxyl group of AmB molecule. The second type of hydrogen bond was not detected in either the AmBCh or AmBER simulation. The large distance between the sterol's hydroxyl and AmB's carboxyl groups makes it almost impossible to form a hydrogen bond between these two groups. On the other hand, intermolecular hydrogen bonds between the sterol hydroxyl group and the AmB amino group were detected in both simulations. Although the number of sterol–AmB hydrogen bonds is not substantial, there are considerable differences in the AmBCh and AmBER simulations (Fig. 9). First, there are more hydrogen bonds in case of the AmBER channel compared to AmBCh. Secondly, the distance between the sterol oxygen atom and the AmB nitrogen atom is almost the same for all pairs of molecules in the AmBER channel. This is not the case for the AmBCh (Fig. 9). We have also monitored the distances between sterol's hydroxyl group and AmB's various groups to investigate if other hydrogen bonds can be formed between these molecules. The chemiketal oxygen atom and hydroxyl groups in the amino-sugar moiety of AmB were traced. It was found that only a limited number of such bonds is formed (one to three out of possible eight), and these intermolecular hydrogen bonds exist only in the case of the AmBER channel (data not shown). These results further indicate that the interaction between cholesterol hydroxyl group and AmB is less specific than the ergosterol hydroxyl group's interaction with the antibiotic.

3.2.4. Relative position of AmB and sterol in the channel

Intermolecular hydrogen bond data presented above show that the relative position of AmB and sterol is different in both types of channels. To further investigate the channel geometry, the following distances between selected carbon

atoms in the rigid parts of AmB and sterol molecules were also tracked: (i) distance between the C9 carbon atom of AmB and the C19 carbon atom of sterol (Figs. 1); and (ii) distance between the C22 carbon atom of AmB and the C19 carbon atom of sterol. Atoms C9 and C22 reside in the opposite fragments of the AmB lactone ring. The selection was made in such a way that comparison of both distances traces the rotation of the sterol's ring system about its long axis as well as up and down movement of sterol molecule relative to AmB molecules. If the C9–C19 and C22–C19 distances are similar, it would mean that the sterol's ring system is aligned parallel with the AmB molecules. The methyl group of the sterol (atom C19) in this case is equally distant from both chains of AmB lactone ring. The values of the traced distances for both types of channels are presented in Fig. 10a–c. In the AmBER channel, the C9–C19 and C22–C19 distances are very similar, roughly around 7 Å, in seven out of eight molecule pairs (Fig. 10b). In contrast, in the AmBCh channel only four out of eight pairs have similar distances, ~ 8 Å, between the C9–C19 and C22–C19 atoms (Fig. 10a). When the C9–C19 and C22–C19 distances differ, the sterol molecules are either rotated along their long axis (relatively to AmB molecule) or the alignment of their long axis with respect to AmB's position is tilted. It was also found that for two of the cholesterol molecules in AmBCh channel the measured distances were around 5 Å. These two cholesterol molecules were shifted along the long axis but, since both measured distances are roughly equal, they were still parallel to their respective AmB molecules. Fig. 10c presents the distribution of states (channels) where position of the cholesterol is rotated using the decision criteria that C9–C19 and C22–C19 distances differ by more than 2 Å. The distributions are roughly the same for both channels. However, one should remember the case of two cholesterol molecules in AmBCh channel with shorter traced distances. Although these molecules are shifted relative to AmB, they are still positioned parallel to the AmBs. All these observations indicate that: (i) the relative positioning of AmB and sterol molecules depends on the sterol type, and

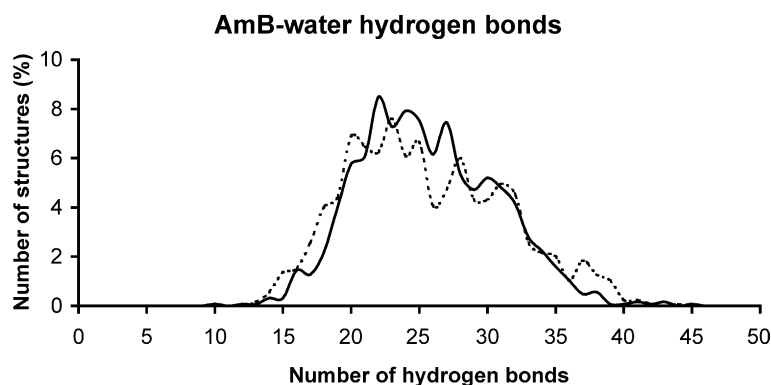


Fig. 11. Distribution of the total number of intermolecular AmB–water hydrogen bonds. Each line indicates the percentage of structures (frames) from the MD simulation trajectory having a particular number of such hydrogen bonds (x-axis). AmBCh channel (solid line); AmBER channel (dashed line).

(ii) the ergosterol “sticks” to AmB better and makes better molecular contact with AmB than the cholesterol in a channel configuration. Different relative positioning of sterols and AmBs may also indirectly influence the interaction between AmB and phospholipid molecules.

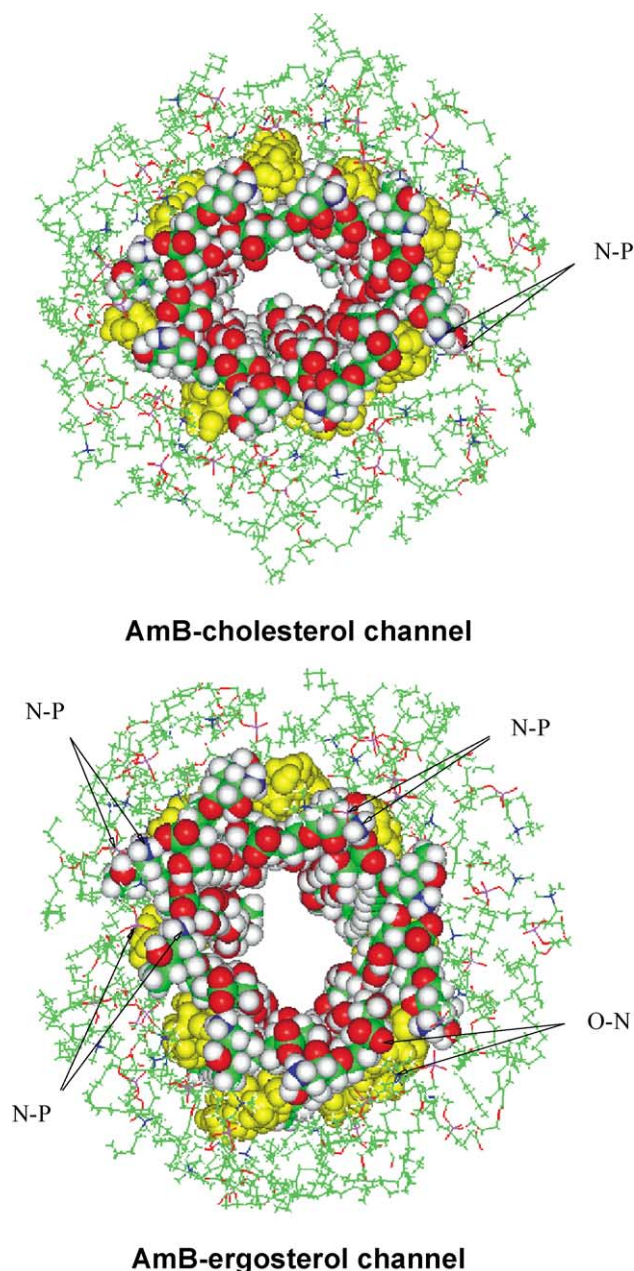


Fig. 12. A snapshot of the AmBCh channel (upper panel), and a snapshot of the AmBER channel (lower panel). Both snapshots are the last frames of the respective MD simulations. AmB and sterol molecules are presented as balls, DMPC molecules as sticks. Sterol molecules are yellow. Black arrows present the accounted AmB–DMPC interactions if the distance between the AmB’s amino nitrogen (blue) and DMPC’s phosphate (pink) atom or between the DMPC’s amino nitrogen (blue) and AmB’s carboxyl oxygen (red) atom is less than 4 Å.

3.2.5. Solvation properties of the channel

The distribution of the number of hydrogen bonds formed between AmB molecules and water molecules is presented in Fig. 11. The waters in the pore form 13 to 40 hydrogen bonds with the channel forming molecules. The most noticeable but probably insignificant difference between the results for the AmBCh and AmBER channels is that the distribution of the number of AmB–water hydrogen bonds has a slightly more pronounced peak in the AmBCh channel. This could be indicating that AmBCh channel has a more steady structure that fluctuates less over time. In the case of the AmBER channel, there are configuration changes that require acquiring new solvation patterns.

3.2.6. Role of the lipids

The presence of explicit lipid molecules in the simulations was necessary not only to better mimic the membrane environment but also to find the possible interactions between AmB or sterols and DMPC molecules. Since only a relatively thin layer of lipids was used, quantitative study of the interactions between AmB or sterols and DMPC molecules would not be reliable. Therefore, we only comment on several interesting observations. The electrostatic interactions between AmB and lipid molecules can be important because AmB and DMPC molecules contain two charged groups each: AmB sugar moiety’s amino and carboxyl groups, and DMPC phosphate and amino groups. Since the intramolecular distance between these two sets of polar groups is roughly equal, formation of a pair of strong ionic bonds between AmB and DMPC is possible. Such bonds were observed in both AmB–sterol channels (Fig. 12), however, these bonds are formed much more often in the AmBER channel (based on selected snapshots from the last 50 ps of the MD simulation). The observed difference may be due to the tighter interaction between AmB and ergosterol relative to AmB and cholesterol. The fact that polar interactions between AmB and DMPC molecules were observed might be indicating that lipids play an active role in channel stability, formation, and destruction.

4. Conclusions

The MD simulations of AmB membrane channels with two different sterols (cholesterol or ergosterol) in the membrane bilayer revealed that AmB channel properties depend on the sterol type. Since the simulations differ only in the molecular structures of the sterols, the differences in the results can be assumed to be mainly due to the differences in the interactions between AmB and sterol molecules. Noting that the AmB membrane channel is a supramolecular complex, it would not be surprising if small variations in local interactions can give rise to important differences in the overall properties.

The main differences between AmBCh and AmBER channels observed during MD simulations can be summarized as follows:

- The diameter of the AmBER channel is larger than that of the AmBCh channel. Since channels are very similar in character, larger pore size implies more efficient transmission of the ions.
- Mutual placement of sterol and AmB molecules is different in the AmBCh and AmBER channels. Ergosterols in the AmBER channel make better contact with the antibiotic molecules and they are more likely to move in accord with AmB molecules than cholesterol. This allows for more favorable van der Waals interactions between ergosterol and AmB molecules. In contrast, cholesterol molecules are more free to move independently and are able to slide up or down along AmB. Such independent movements often break the possible short-range van der Waals interactions between cholesterol and AmB molecules in the AmBCh channel.
- Intermolecular hydrogen bonds between amino and carboxyl groups of neighboring AmB molecules are formed more efficiently in the AmBER channel.
- Formation of intermolecular hydrogen bonds between sterol's hydroxyl group and AmB amino group is more pronounced in the AmBER channel.
- Interactions between DMPC polar groups and AmB amino or carboxyl groups are more pronounced in the AmBER channel.

Because of the observations listed above, our MD simulation results support the expectation that the AmBER channel is more stable than the AmBCh channel. These observations are consistent with sterol hypothesis of selective toxicity of AmB, and also support the experimental efforts leading to obtain new sterically hindered derivatives synthesized by modifying the amino group of AmB's amino-sugar moiety (e.g., Refs. [38,60]). These new derivatives bear large substituents at the amino group site, and they are particularly designed to block the intermolecular hydrogen bond ring formed at the pore entrance. Breaking of the hydrogen bond network modifies AmB and sterol molecules' freedom of movement and, as a result, can have a strong impact on the short range interactions due to the molecular contact [17]. As implied in our simulation results, having better contact between AmB and sterols is important in increasing the stability of the membrane ion channel. As a consequence, the changes in the channel structure affecting the AmB's molecular contact with the sterols could be defining the toxicity of AmB's derivatives.

Acknowledgements

This work was supported by The State Committee of Scientific Research, Warsaw (Poland) (grant number

3T09A07014) and partially by Technical University of Gdansk. We also thank the ICM Computational Center in Warsaw (Poland) for granting computation time on the Cray T3E machine.

References

- [1] H.A. Gallis, R.H. Drew, W.W. Pickard, *Rev. Infect. Dis.* 12 (1990) 308–329.
- [2] S. Hartsel, J. Bolard, *Trends Pharmacol. Sci.* 17 (1996) 445–449.
- [3] M.A. Ghanoun, L.B. Rice, *Clin. Microbiol. Rev.* 12 (1999) 501.
- [4] S.Y. Ablordeppey, P.C. Fan, J.H. Ablordeppey, L. Mardenborough, *Curr. Med. Chem.* 6 (1999) 1151–1195.
- [5] S.E. Vartivarian, E.J. Anaissie, G.P. Bodey, *Clin. Infect. Dis.* 17 (1993) S487–S491.
- [6] O. Lortholary, B. Dupont, *Clin. Microbiol. Rev.* 10 (1997) 477.
- [7] A.M. Hillery, *Adv. Drug Deliv. Rev.* 24 (1997) 345–363.
- [8] B. De Kruijff, R.A. Demel, *Biochim. Biophys. Acta* 339 (1974) 57–70.
- [9] J. Bolard, *Biochim. Biophys. Acta* 864 (1986) 257–304.
- [10] J. Brajtburg, W.G. Powderly, G.S. Kobayashi, G. Medoff, *Antimicrob. Agents Chemother.* 34 (1990) 183–188.
- [11] S.C. Hartsel, C. Hatch, W. Ayenew, J. Liposome Res. 3 (1993) 377–408.
- [12] J.M.T. Hamilton-Miller, *Adv. Appl. Microbiol.* 17 (1974) 109–134.
- [13] T. Teerlink, B. De Kruijff, R.A. Demel, *Biochim. Biophys. Acta* 599 (1980) 484–492.
- [14] B.V. Cotero, S. Rebollo Antunez, I. Ortega-Blake, *Biochim. Biophys. Acta* 1375 (1998) 43–51.
- [15] D. Kerridge, *Adv. Microb. Physiol.* 27 (1986) 1–72.
- [16] I. Fournier, J. Barwicz, P. Tancrede, *Biochim. Biophys. Acta* 1373 (1998) 76–86.
- [17] M. Herve, J.C. Debouzy, E. Borowski, B. Cybulska, C.M. Gary-Bobo, *Biochim. Biophys. Acta* 980 (1989) 261–272.
- [18] M. Baginski, Doctoral thesis, Gdansk, 1995.
- [19] M. Baginski, A. Tempezyk, E. Borowski, *Eur. Biophys. J.* 17 (1989) 159–166.
- [20] M. Baginski, E. Borowski, *J. Mol. Struct., Theochem* 389 (1997) 139–146.
- [21] M. Baginski, P. Bruni, E. Borowski, *J. Mol. Struct., Theochem* 311 (1994) 285–296.
- [22] A. Marty, A. Finkelstein, *J. Gen. Physiol.* 65 (1975) 515–526.
- [23] P. VanHoogevest, B. de Kruijff, *Biochim. Biophys. Acta* 511 (1978) 397–407.
- [24] J. Berges, J. Caillet, J. Langlet, N. Gresh, M. Herve, C.M. Gary-Bobo, *Stud. Phys. Theor. Chem.* 71 (1990) 253–263.
- [25] M. Bonilla-Marin, M. Moreno-Bello, I. Ortega-Blake, *Biochim. Biophys. Acta* 1061 (1991) 65–77.
- [26] S. Meddeb, J. Berges, J. Caillet, J. Langlet, *Biochim. Biophys. Acta* 1112 (1992) 266–272.
- [27] V.E. Khutorsky, *Biochim. Biophys. Acta* 1108 (1992) 123–127.
- [28] M. Baginski, P. Gariboldi, E. Borowski, *Biophys. Chemist.* 49 (1994) 241–250.
- [29] V. Khutorsky, *Biophys. J.* 71 (1996) 2984–2995.
- [30] J. Mazerski, E. Borowski, *Biophys. Chemist.* 57 (1996) 205–217.
- [31] M. Baginski, P. Gariboldi, P. Bruni, E. Borowski, *Biophys. Chemist.* 65 (1997) 91–100.
- [32] M. Baginski, H. Resat, J.A. McCammon, *Mol. Pharmacol.* 52 (1997) 560–570.
- [33] A. Silberstein, *J. Membr. Biol.* 162 (1998) 117–126.
- [34] H. Resat, F.A. Sungur, M. Baginski, E. Borowski, V. Aviyente, *J. Comput.-Aided Mol. Des.* 14 (2000) 689–703.
- [35] S.E. Feller, *Curr. Opin. Colloid Interface Sci.* 5 (2000) 217–223.
- [36] M.S.P. Sansom, I.H. Shrivastava, K.M. Ranatunga, G.R. Smith, *Trends Biochem. Sci.* 25 (2000) 368–374.

- [37] L.R. Forrest, M.S.P. Sansom, *Curr. Opin. Struct. Biol.* 10 (2000) 174–181.
- [38] B. Cybulska, I. Gadowska, J. Mazerski, J. Grzybowska, E. Borowski, M. Cheron, J. Bolard, *Acta Biochim. Pol.* 47 (2000) 121–131.
- [39] J. Szlinder-Richert, B. Cybulska, J. Grzybowska, E. Borowski, R. Prasad, *Acta Biochim. Pol.* 47 (2000) 133–140.
- [40] J. Szlinder-Richert, J. Mazerski, B. Cybulska, J. Grzybowska, E. Borowski, *Biochim. Biophys. Acta* 1528 (2001) 15–24.
- [41] P. Ganis, G. Avitabile, W. Mechlinski, C.P. Schaffner, *J. Am. Chem. Soc.* 93 (1971) 4560–4564.
- [42] S.E. Hull, M.M. Woolfson, *Acta Crystallogr., B* 32 (1976) 2370–2373.
- [43] H.S. Shieh, L.G. Hoard, C.E. Nordman, *Acta Crystallogr., B* 37 (1981) 1538–1543.
- [44] T.E. Andreoli, *Kidney Int.* 4 (1973) 337–345.
- [45] E.J. Dufourc, J.C.P. Smith, H.D. Jarrell, *Biochim. Biophys. Acta* 776 (1984) 317–329.
- [46] S.C. Hartsel, S.K. Benz, R.P. Peteron, B.S. Whyte, *Biochemistry* 30 (1991) 77–82.
- [47] A.R. Balakrishnan, K.R.K. Easwaran, *Biochemistry* 32 (1993) 4139–4144.
- [48] I.B. Golovanov, I.G. Tsygankova, *Membr. Cell Biol.* 9 (1995) 335–346.
- [49] E.J. Dufourc, J.C.P. Smith, H.D. Jarrell, *Biochim. Biophys. Acta* 778 (1984) 435–442.
- [50] A.F. DiGiorgio, S. Otto, P. Bandyopadhyay, S.L. Regen, *J. Am. Chem. Soc.* 122 (2000) 11029–11030.
- [51] H. Resat, M. Baginski, *Eur. Biophys. J.* 31 (2002) 294–305.
- [52] B. De Kruijff, W.J. Gerritsen, A. Oerlemans, R.A. Demel, L.L.M. VanDeenen, *Biochim. Biophys. Acta* 339 (1974) 30–43.
- [53] A.J. Robinson, W.G. Richards, P.J. Thomas, M.M. Hann, *Biophys. J.* 67 (1994) 2345–2354.
- [54] B.R. Brooks, R.E. Bruccoleri, B.D. Olafson, D.J. States S. Swaminathan, M. Karplus, *J. Comput. Chem.* 4 (1983) 187–217.
- [55] M. Schlenkerich, J. Brickmann, A.D. MacKerell, M. Karplus, An empirical potential energy function for phospholipids: criteria for parameter optimization and application, in: K.M. Merz, B. Roux (Eds.), *Biological Membranes*, Birkhauser, Boston, 1996, pp. 31–82.
- [56] W.L. Jorgensen, J. Chandrasekhar, J.D. Madura, R.W. Impey, M.L. Klein, *J. Chem. Phys.* 79 (1983) 926–935.
- [57] J. Breed, R. Sankararamakrishnan, I.D. Kerr, M.S.P. Sansom, *Biophys. J.* 70 (1996) 1643–1661.
- [58] A.M. Smondyrev, M.L. Berkowitz, *Biophys. J.* 80 (2001) 1649–1658.
- [59] C.M. Cortis, R.A. Friesner, *J. Comput. Chem.* 18 (1997) 1591–1608.
- [60] J. Grzybowska, P. Sowinski, J. Gumieniak, T. Zieniawa, E. Borowski, *J. Antibiot.* 50 (1997) 709–711.